

# Elliptic flow of $\Lambda$ hyperons in Pb+Pb collisions at 158A GeV

C. Alt,<sup>9</sup> T. Anticic,<sup>21</sup> B. Baatar,<sup>8</sup> D. Barna,<sup>4</sup> J. Bartke,<sup>6</sup> L. Betev,<sup>10</sup> H. Białkowska,<sup>19</sup> C. Blume,<sup>9</sup> B. Boimska,<sup>19</sup> M. Botje,<sup>1</sup> J. Bracinik,<sup>3</sup> R. Bramm,<sup>9</sup> P. Bunčić,<sup>10</sup> V. Cerny,<sup>3</sup> P. Christakoglou,<sup>2</sup> O. Chvala,<sup>15</sup> J.G. Cramer,<sup>17</sup> P. Csató,<sup>4</sup> P. Dinkelaker,<sup>9</sup> V. Eckardt,<sup>14</sup> D. Flierl,<sup>9</sup> Z. Fodor,<sup>4</sup> P. Foka,<sup>7</sup> V. Friese,<sup>7</sup> J. Gál,<sup>4</sup> M. Gaździcki,<sup>9,12</sup> G. Georgopoulos,<sup>2</sup> E. Gładysz,<sup>6</sup> K. Grebieszko,<sup>22</sup> S. Hegyi,<sup>4</sup> C. Höhne,<sup>13</sup> K. Kadija,<sup>21</sup> A. Karev,<sup>14</sup> M. Kliemant,<sup>9</sup> S. Kniege,<sup>9</sup> V.I. Kolesnikov,<sup>8</sup> E. Kornas,<sup>6</sup> R. Korus,<sup>12</sup> M. Kowalski,<sup>6</sup> I. Kraus,<sup>7</sup> M. Kreps,<sup>3</sup> A. Laszlo,<sup>4</sup> M. van Leeuwen,<sup>1</sup> P. Lévai,<sup>4</sup> L. Litov,<sup>18</sup> B. Lungwitz,<sup>9</sup> M. Makariev,<sup>18</sup> A.I. Malakhov,<sup>8</sup> M. Mateev,<sup>18</sup> G.L. Melkumov,<sup>8</sup> A. Mischke,<sup>7</sup> M. Mitrovski,<sup>9</sup> J. Molnár,<sup>4</sup> St. Mrówczyński,<sup>12</sup> V. Nikolic,<sup>21</sup> G. Pál, <sup>4</sup> A.D. Panagiotou,<sup>2</sup> D. Panayotov,<sup>18</sup> A. Petridis,<sup>2</sup> M. Pikna,<sup>3</sup> D. Prindle,<sup>17</sup> F. Pühlhofer,<sup>13</sup> R. Renfordt,<sup>9</sup> C. Roland,<sup>5</sup> G. Roland,<sup>5</sup> M. Rybczyński,<sup>12</sup> A. Rybicki,<sup>6</sup> A. Sandoval,<sup>7</sup> N. Schmitz,<sup>14</sup> T. Schuster,<sup>9</sup> P. Seyboth,<sup>14</sup> F. Siklér,<sup>4</sup> B. Sitar,<sup>3</sup> E. Skrzypczak,<sup>20</sup> G. Stefanek,<sup>12</sup> R. Stock,<sup>9</sup> C. Strabel,<sup>9</sup> H. Ströbele,<sup>9</sup> T. Susa,<sup>21</sup> I. Szentpétery,<sup>4</sup> J. Sziklai,<sup>4</sup> P. Szymanski,<sup>10,19</sup> V. Trubnikov,<sup>19</sup> D. Varga,<sup>4,10</sup> M. Vassiliou,<sup>2</sup> G.I. Veres,<sup>4,5</sup> G. Vesztegombi,<sup>4</sup> D. Vranić,<sup>7</sup> A. Wetzler,<sup>9</sup> Z. Włodarczyk,<sup>12</sup> A. Wojtaszek,<sup>12</sup> I.K. Yoo,<sup>16</sup> and J. Zimányi<sup>4</sup>

(The NA49 collaboration)

<sup>1</sup>NIKHEF, Amsterdam, Netherlands.

<sup>2</sup>Department of Physics, University of Athens, Athens, Greece.

<sup>3</sup>Comenius University, Bratislava, Slovakia.

<sup>4</sup>KFKI Research Institute for Particle and Nuclear Physics, Budapest, Hungary.

<sup>5</sup>MIT, Cambridge, USA.

<sup>6</sup>The H.Niewodniczanski Institute of Nuclear Physics, Polish Academy of Sciences, Cracow, Poland.

<sup>7</sup>Gesellschaft für Schwerionenforschung (GSI), Darmstadt, Germany.

<sup>8</sup>Joint Institute for Nuclear Research, Dubna, Russia.

<sup>9</sup>Fachbereich Physik der Universität, Frankfurt, Germany.

<sup>10</sup>CERN, Geneva, Switzerland.

<sup>11</sup>University of Houston, Houston, TX, USA.

<sup>12</sup>Institute of Physics Świętokrzyska Academy, Kielce, Poland.

<sup>13</sup>Fachbereich Physik der Universität, Marburg, Germany.

<sup>14</sup>Max-Planck-Institut für Physik, Munich, Germany.

<sup>15</sup>Institute of Particle and Nuclear Physics, Charles University, Prague, Czech Republic.

<sup>16</sup>Department of Physics, Pusan National University, Pusan, Republic of Korea.

<sup>17</sup>Nuclear Physics Laboratory, University of Washington, Seattle, WA, USA.

<sup>18</sup>Atomic Physics Department, Sofia University St. Kliment Ohridski, Sofia, Bulgaria.

<sup>19</sup>Institute for Nuclear Studies, Warsaw, Poland.

<sup>20</sup>Institute for Experimental Physics, University of Warsaw, Warsaw, Poland.

<sup>21</sup>Rudjer Boskovic Institute, Zagreb, Croatia.

<sup>22</sup>Warsaw University of Technology, Warsaw, Poland.

The elliptic flow of  $\Lambda$  hyperons has been measured by the NA49 experiment at the CERN-SPS in semi-central Pb+Pb collisions at 158A GeV. The standard method of correlating particles with the event plane was used. Measurements of  $v_2$  near mid-rapidity are reported as a function of rapidity, centrality and transverse momentum. Elliptic flow of  $\Lambda$  particles increases both with the impact parameter and with the transverse momentum. It is compared with  $v_2$  for pions and protons as well as with model calculations. The observation of large elliptic flow and its mass dependence suggest strong collective behaviour of the matter produced in collisions of heavy nuclei already at the SPS.

PACS numbers: 25.75.Ld

Elliptic flow has its origin in the spatial anisotropy of the initial reaction volume in non-central collisions and in particle rescatterings in the evolving system which convert the spatial anisotropy into a momentum anisotropy [1]. The spatial anisotropy decreases rapidly because of the fast expansion of the system [2] making the momentum anisotropy measured at the end of this evolution strongly dependent on the matter properties and the effective equation of state (EoS) at the early stage [3, 4]. Comparison of measured anisotropies with hydro-

dynamic model calculations provide an important test of the degree of thermalisation in the produced particle system. Flow of heavy particles is affected more strongly by changes in the EoS than flow of pions [4, 5, 6]. Moreover, various hadron types are believed to decouple at different times and with different temperatures [7]. Thus the elliptic flow of various particle species allows insight into different stages of the collision.

The anisotropic flow parameters measured to date at SPS and lower energies are mainly those of pions and

protons [8, 9]. RHIC experiments have measured elliptic flow for many particle species [10], including hyperons [10, 11]. In these experiments, the rapid rise of elliptic flow with transverse momentum  $p_T$  up to 1.5 GeV/c and its particle-mass dependence are well reproduced by hydrodynamic models [10]. In order to test the validity of this scenario at SPS energies we have extended elliptic flow measurements in 158A GeV Pb+Pb ( $\sqrt{s_{NN}} = 17.2$  GeV) collisions to  $\Lambda$  hyperons. Although  $\Lambda$  particles have a smaller detection efficiency than protons, they are less affected by feeddown from resonance and weak decays. In this paper, results on  $\Lambda$  elliptic flow as a function of the center of mass rapidity  $y$  and transverse momentum  $p_T$  will be presented and compared to model calculations.

The main components of the NA49 detector [12] are four large-volume Time Projection Chambers for tracking and particle identification by  $dE/dx$  measurement with a resolution of 3–6%. The TPC system consists of two vertex chambers inside the spectrometer magnets and two main chambers placed behind the magnets at both sides of the beam. Downstream of the TPCs a veto calorimeter detects projectile spectators and is used for triggering and centrality selection. The data sample consists of  $3 \times 10^6$  semi-central Pb+Pb events after on-line trigger selection of the 23.5% most central collisions. The events were divided into three different centrality bins, which correspond to the first three bins used in a previous analysis (see Table 1 in [9]) and are defined by centrality ranges 0–5% (bin 1), 5–12.5% (bin 2), and 12.5–23.5% (bin 3). Many model predictions are published for certain impact parameter ranges which are: 0–3.4 fm (bin 1), 3.4–5.3 fm (bin 2), and 5.3–7.4 fm (bin 3) for our centrality classes. The measurement in the centrality range  $\sigma/\sigma_{TOT} = 5$ –23.5% (called mid-central) is obtained by averaging the results of bins 2 plus 3 with weights corresponding to the fractions of the total cross section in these bins.

The  $\Lambda$  hyperon candidates were selected from the sample of  $V^0$ -track configurations consisting of oppositely charged particles, which include the  $\Lambda$  decays into proton and  $\pi^-$  (branching ratio 63.9%). The identification method [13] relies on the evaluation of the invariant mass distribution and is enhanced by daughter particle identification applying a cut in  $dE/dx$  around the expectation value derived from a Bethe-Bloch parametrization. The yields of  $\Lambda$  hyperons are obtained by counting the number of entries in the invariant mass peak above the estimated background as a function of the azimuthal angle  $\phi_{lab}$  with respect to the event plane (see below). The background is estimated from a fit of invariant mass spectra to the sum of a Lorentz distribution and a polynomial. The extracted  $\Lambda$  candidates have a background contamination of 5–9% in the  $\Lambda$  mass window 1.108–1.124 GeV/ $c^2$ , depending on centrality. The acceptance of  $\Lambda$  hyperons covers the range  $0.4 \lesssim p_T \lesssim 4$  GeV/c and  $-1.5 \lesssim y \lesssim 1.0$  and strongly depends on  $p_T$  and  $y$ . Multiplicative fac-

tors were introduced for every  $\Lambda$  particle to correct the  $\Lambda$  yields for detector and reconstruction efficiency. They were determined as ratios of theoretical  $\Lambda$  yields from Blast Wave parametrization ( $T = 84$  MeV,  $\langle\beta_T\rangle \approx 0.5$ ) to the measured yields.

The elliptic flow analysis is based on the standard procedure outlined in [9, 14] to reconstruct the event plane for each event and the corrections for the event plane resolution. The event plane is an experimental estimator of the true reaction plane and is calculated from the azimuthal distribution of primary charged  $\pi$  mesons. Identification of pions is based on energy loss measurements ( $dE/dx$ ) in the TPCs. To avoid possible auto-correlations, tracks associated with  $\Lambda$  candidates are excluded from the event plane calculation. The method to determine the event plane angle  $\Phi_{2EP}$  uses the elliptic flow of pions, according to the formula:

$$\begin{aligned} X_2 &= \sum_{i=1}^N p_T^i [\cos(2\phi_{lab}^i) - \langle\cos(2\phi_{lab})\rangle], \\ Y_2 &= \sum_{i=1}^N p_T^i [\sin(2\phi_{lab}^i) - \langle\sin(2\phi_{lab})\rangle], \\ \Phi_{2EP} &= \tan^{-1} \left( \frac{Y_2}{X_2} \right) / 2. \end{aligned} \quad (1)$$

where  $X_2, Y_2$  are the components of the event plane flow vector  $\mathbf{Q}_2$  and the sums run over accepted charged pion tracks. The acceptance correction is based on the recentering method of [9] which consists of subtracting in Eq.1 the mean values  $\langle\cos(2\phi_{lab})\rangle$  and  $\langle\sin(2\phi_{lab})\rangle$ . These mean values are calculated in bins of  $p_T$  and rapidity for all pions in those events which contain at least one  $\Lambda$  hyperon candidate. The means were stored in a 3-dimensional matrix of 20  $p_T$  intervals, 50 rapidity intervals, and eight centrality bins. A second level acceptance correction is done by using mixed events. We used 10 mixed events for each real event. Particles for mixed events are randomly selected from different events in the same centrality bin with at least one  $\Lambda$  hyperon. The final angular distributions are obtained by dividing the real  $\Lambda$  angular distributions by the mixed event distributions to remove the acceptance correlations remaining after recentering. The corrected  $\Lambda$  azimuthal distributions are then fitted with a truncated Fourier series:

$$\begin{aligned} \frac{dN}{d(\phi_{lab} - \Phi_{2EP})} &= \\ &\text{const} \times (1 + v_2^{obs} \cos[2(\phi_{lab} - \Phi_{2EP})] \\ &\quad + v_4^{obs} \cos[4(\phi_{lab} - \Phi_{2EP})]). \end{aligned} \quad (2)$$

The elliptic flow  $v_2$  is evaluated by dividing the observed anisotropy  $v_2^{obs}$  by the event plane resolution  $R$ :

$$v_2 = \frac{v_2^{obs}}{R}. \quad (3)$$

The event plane resolution,

$$R = \langle \cos[2(\Phi_{2EP} - \Phi_r)] \rangle = \sqrt{2 \langle \cos[2(\Phi_{2EP}^a - \Phi_{2EP}^b)] \rangle},$$

is calculated from the correlation of two planes ( $\Phi_{2EP}^a, \Phi_{2EP}^b$ ) for random sub-events with equal multiplicity. The results are  $R = 0.27, 0.34$  and  $0.40$  for centrality bins 1, 2 and 3, respectively. The uncertainty due to the background subtraction, event plane resolution and the mixed event corrections are added to the total error in Figs. 2-4. The observed hexadecupole anisotropy  $v_4^{obs}$  is consistent with zero within statistical errors for all centrality bins. The final statistics in our sample consists

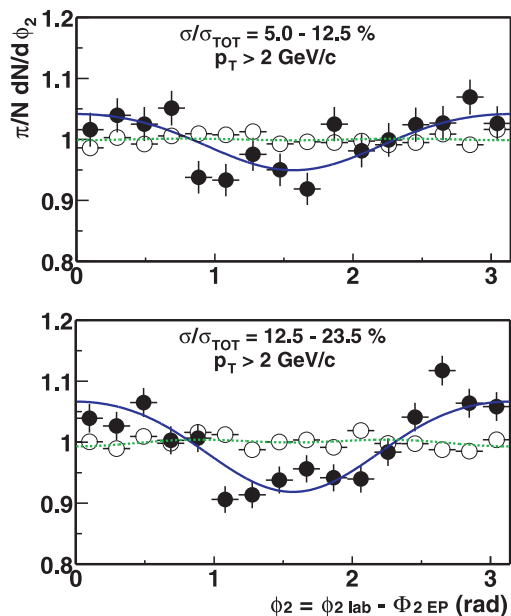


FIG. 1: Azimuthal distributions of  $\Lambda$  hyperons with respect to the event plane for real events (solid symbols) and mixed-events (open symbols) in two centrality bins. The curves are Fourier expansion fits (see text Eq. (2)).

of about  $10^6$   $\Lambda$  candidates. This allows flow analysis for several rapidity and  $p_T$  bins.

In Fig. 1 are shown the azimuthal distributions of  $\Lambda$  hyperons with respect to the estimated reaction plane for real and mixed events. The curves represent results of fits with the truncated Fourier series Eq. (2). The distributions exhibit a strong correlation for real events (full symbols and curves). As expected, no correlation is observed for mixed-events (open symbols, dashed curves). The correlation significantly increases with transverse momentum (shown in Fig. 2) and with impact parameter. The  $p_T$  averaged elliptic flow is obtained from all identified  $\Lambda$  hyperons without  $p_T$  cuts. It exhibits no significant dependence on rapidity as shown in Fig. 2(top). The absence of a rapidity dependence of  $v_2(y)$  was also observed for protons (see Fig. 6 of [9]) in mid-central

events. The flatness of  $v_2(y)$  allows to use the  $\Lambda$  sample from the full rapidity range of the data in Fig. 2(top) for the study of  $v_2$  as a function of  $p_T$ .

The  $p_T$  dependence of rapidity-averaged  $\Lambda$  elliptic flow is shown in the bottom plot of Fig. 2 for two centrality ranges. The  $v_2$  parameter significantly increases with transverse momentum, the rise being stronger for more peripheral events. Fig. 3 shows a comparison of  $v_2(p_T)$

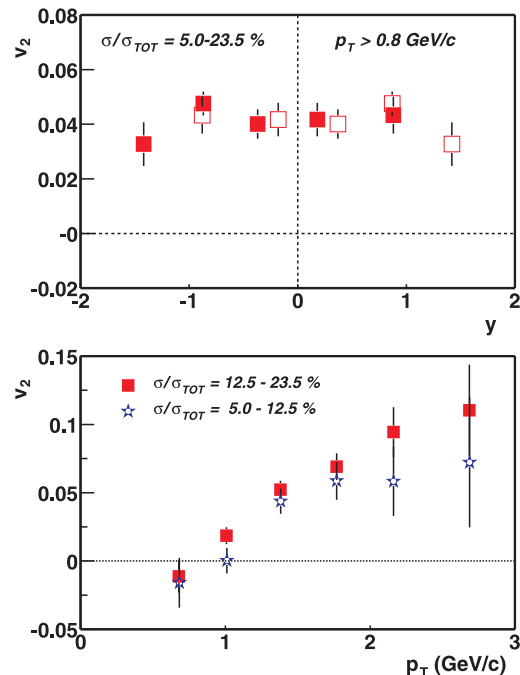


FIG. 2: Elliptic flow of  $\Lambda$  hyperons as a function of rapidity (top) and  $p_T$  (bottom). The open points in the top graph have been reflected about midrapidity.

of  $\Lambda$  hyperons for mid-central and central (0-5%) events measured by the NA49 and STAR experiments [15]. The NA45 collaboration recently also presented preliminary results in Pb+Au collisions at the top SPS energy [16] which agree well with the NA49 results (not shown). For mid-central collisions at SPS energy the elliptic flow grows linearly with  $p_T$  up to  $\sim 2$  GeV/c, but the increase is steeper at RHIC than at SPS energy. It should be noted that RHIC mid-central data have been measured in the centrality range  $\sigma/\sigma_{TOT} = 5-30\%$  while SPS events are somewhat more central. The effect of different centrality ranges has been estimated by hydrodynamic calculations [17] at RHIC energy for the slightly different centrality bins of NA49 and STAR. As shown by the corresponding curves in Fig. 3 this explains only partly the difference between both measurements. For central collisions NA49 measurements also seem to show lower values of  $v_2$  than STAR.

A comparison of  $v_2(p_T)$  for pions, protons and  $\Lambda$  hyperons as measured by the NA49 experiment in mid-central

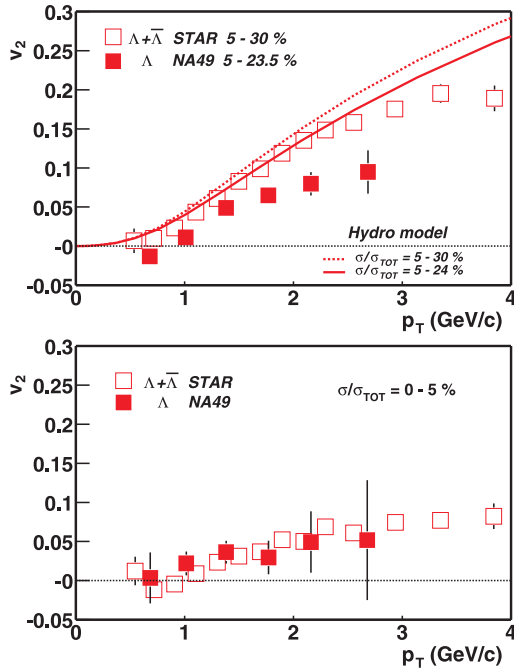


FIG. 3: Elliptic flow of  $\Lambda$  hyperons as a function of  $p_T$  from mid-central (top) and central (bottom) events measured by the STAR (open symbols) and NA49 (solid symbols) experiments. Curves are hydrodynamical model predictions at RHIC energy for the two different centrality bins.

events is displayed in Fig. 4. The values for pions and protons were obtained as the cross section weighted averages of the measurements published in [9] for the appropriate centrality range. As seen in Fig. 4 the elliptic flow grows linearly with  $p_T$  for all particle species but the rise for pions starts from  $p_T$  close to zero while for protons and  $\Lambda$  particles it starts from  $p_T \approx 0.5$  GeV/c. The elliptic flow for pions is significantly larger than that for heavier particles although at  $p_T \approx 2$  GeV/c the flow becomes similar for all particle species. Data are reproduced by blast wave fits [5, 18] (curves in Fig. 4(top)) with the following parameters: freeze-out temperature  $T = 92$  MeV, mean transverse expansion rapidity  $\rho_0 = 0.82$ , and its second harmonic azimuthal modulation amplitude  $\rho_a = 0.021$ . The values are similar to those obtained by simultaneous fitting of  $p_T$  spectra and HBT radii [19].

In Fig. 4(bottom) the measured values of  $v_2$  are compared to hydrodynamical model calculations [20] assuming a first-order phase transition to a QGP at the critical temperature  $T_c = 165$  MeV. With the freeze-out temperature  $T_f = 120$  MeV tuned to reproduce particle spectra, the model calculations significantly overestimate the SPS results for semi-central collisions (full curves in Fig. 4(bottom)) in contradiction to predictions at RHIC energy which agree with data quite well for  $p_T \lesssim 2$  GeV/c [15] (not shown). The discrepancy at SPS may indicate a lack of complete thermalisation or a vis-

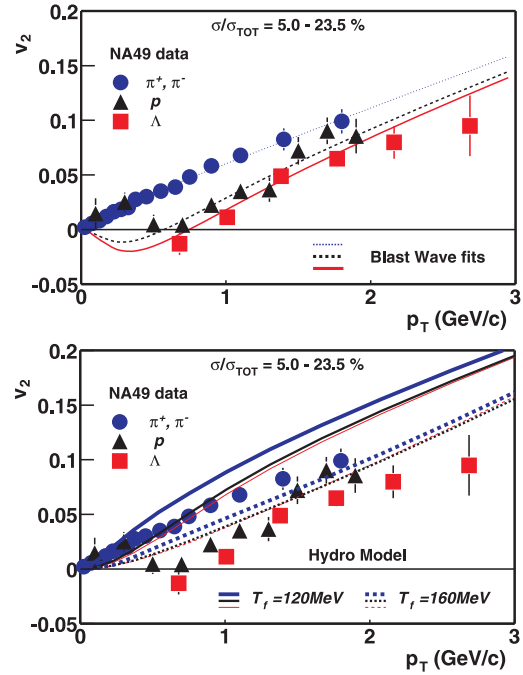


FIG. 4: Elliptic flow for charged pions (circles), protons (triangles) and  $\Lambda$  hyperons (squares) as a function of  $p_T$  from 158A GeV Pb+Pb mid-central events measured by the NA49 experiment. Curves are blast wave fits (top) and hydrodynamical model predictions for two freeze-out temperatures at SPS energy (bottom).

cosity effect. On the other hand, the model reproduces qualitatively the characteristic hadron-mass ordering of elliptic flow. Thus the data support the hypothesis of early development of collectivity. The calculation from the same model with a higher temperature  $T_f = 160$  MeV exhibits better agreement with the  $\Lambda$  flow data (dotted curves in Fig. 4(bottom)). Unfortunately, the model does not simultaneously reproduce the  $m_T$  spectra with such a high freeze-out temperature. A solution of this problem was found by coupling a hadronic rescattering phase to the hydrodynamical evolution and hadronisation [4]. This model can reproduce  $m_T$  spectra and elliptic flow both at top SPS energy and RHIC consistently, although predictions of  $v_2$  for exactly the centrality range of the present analysis are not published in the literature. One should note, however, that none of the hydrodynamical models have yet been able to describe Bose-Einstein correlations successfully.

In summary, we have reported the first measurement of the anisotropic flow parameter  $v_2$  for  $\Lambda$  particles from Pb+Pb collisions at  $\sqrt{s_{NN}} = 17.2$  GeV. Elliptic flow of  $\Lambda$  hyperons exhibits no significant dependence on rapidity for  $-1.5 \lesssim y \lesssim 1.0$ . It rises linearly with  $p_T$  and is smaller than  $v_2$  for pions. Both features are well reproduced by the Blast Wave parametrization and the hydrodynamic model. The increase of  $v_2$  with  $p_T$  is weaker at SPS

than at RHIC energy. The observation of large elliptic flow and its mass dependence suggest strong collective behaviour of the matter produced in collisions of heavy nuclei already at the SPS. Hydrodynamic models with a deconfinement phase transition and a microscopic freeze-out treatment appear to provide a consistent description of  $v_2$  and  $m_T$  spectra at both top SPS and RHIC energies.

This work was supported by the US Department of Energy Grant DE-FG03-97ER41020/A000, the Bundesministerium für Bildung und Forschung 06F-137, Germany, the Virtual Institute VI-146 of Helmholtz Gemeinschaft, Germany, the Polish State Committee for Scientific Research (1 P03B 006 30, 1 P03B 097 29, 1 P03B 121 29, 1 P03B 127 30), the Hungarian Scientific Research Foundation (T032648, T032293, T043514), the Hungarian National Science Foundation, OTKA, (F034707), the Polish-German Foundation, the Korea Science & Engineering Foundation (R01-2005-000-10334-0) and the Bulgarian National Science Fund (Ph-09/05).

---

[1] J. Y. Ollitrault, Nucl. Phys. A **638**, 195 (1998).  
 [2] P. F. Kolb, J. Sollfrank and U. W. Heinz, Phys. Rev. C **62**, 054909 (2000).  
 [3] J. Y. Ollitrault, Phys. Rev. D **46**, 229 (1992); H. Sorge, Phys. Rev. Lett. **82**, 2048 (1999).  
 [4] D. Teaney, J. Lauret and E. V. Shuryak, Phys. Rev. Lett. **86**, 4783 (2001) and nucl-th/0110037.  
 [5] P. Huovinen, P. F. Kolb, U. W. Heinz, P. V. Ruuskanen and S. A. Voloshin, Phys. Lett. B **503**, 58 (2001).

[6] R. Snellings [STAR Collaboration], Heavy Ion Phys. **21**, 237 (2004).  
 [7] H. van Hecke, H. Sorge and N. Xu, Phys. Rev. Lett. **81**, 5764 (1998).  
 [8] N. Bastid *et al.* [FOPI Collaboration], Nucl. Phys. A **622**, 573 (1997); A. Andronic *et al.* [FOPI Collaboration], Nucl. Phys. A **679**, 765 (2001); J. Barrette *et al.* [E877 Collaboration], Phys. Rev. C **55**, 1420 (1997); H. Appelshauser *et al.* [NA49 Collaboration], Phys. Rev. Lett. **80**, 4136 (1998).  
 [9] C. Alt *et al.* [NA49 Collaboration], Phys. Rev. C **68**, 034903 (2003).  
 [10] J. Adams *et al.* [STAR Collaboration], Phys. Rev. C **72**, 014904 (2005).  
 [11] J. Adams *et al.* [STAR Collaboration], Phys. Rev. Lett. **95**, 122301 (2005).  
 [12] S. V. Afanasiev *et al.* [NA49 Collaboration], Nucl. Instr. Meth. A **430**, 210 (1999).  
 [13] H. Appelshauser *et al.* [NA49 Collaboration], J. Phys. G **25**, 469 (1999); L.S. Barnby, Ph.D. Thesis, University of Birmingham (1999).  
 [14] S. A. Voloshin and A. M. Poskanzer, Phys. Lett. B **474**, 27 (2000).  
 [15] J. Adams *et al.* [STAR Collaboration], Phys. Rev. Lett. **92**, 052302 (2004).  
 [16] J. Milosević *et al.* [NA45 Collaboration], nucl-ex/0510057 (2005).  
 [17] P. Huovinen, Nucl. Phys. A **761**, 296 (2005), and private communication.  
 [18] C. Adler *et al.* [STAR Collaboration], Phys. Rev. Lett. **87**, 182301 (2001).  
 [19] S. Kniege *et al.* [NA49 Collaboration], nucl-ex/0601024 (2006).  
 [20] P. Huovinen, private communication (2005),  $T_c = 165$  MeV,  $T_f = 120, 160$  MeV, EoS=Q.